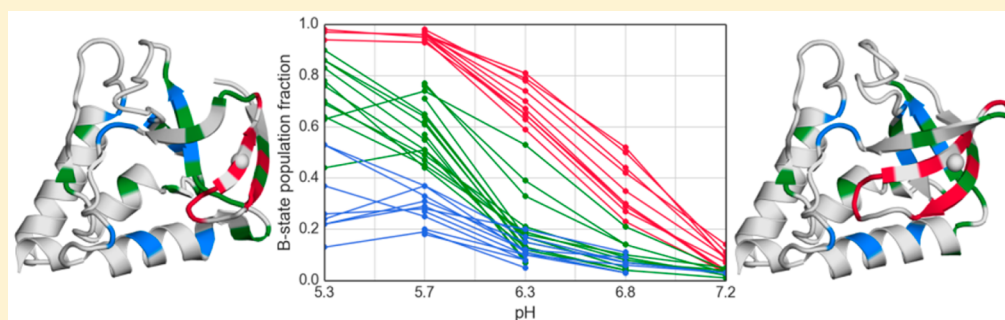


Conformational Reorganization Coupled to the Ionization of Internal Lys Residues in Proteins

Daniel E. Richman,[†] Ananya Majumdar,[‡] and Bertrand García-Moreno E.^{*,†}

[†]Department of Biophysics and [‡]Biomolecular NMR Center, Johns Hopkins University, 3400 North Charles Street, Baltimore, Maryland 21218, United States

S Supporting Information



ABSTRACT: Ionizable groups buried in the hydrophobic interior of proteins are essential for energy transduction and catalysis. Because the protein interior is usually neither as polar nor as polarizable as water, these groups tend to have anomalous pK_a values, and their ionization tends to be coupled to conformational reorganization. To elucidate mechanisms of energy transduction in proteins, it is necessary to understand the structural determinants of the pK_a values of these buried groups, including the range and character of the conformational reorganization that the ionization of these buried groups can elicit. The L25K and L125K variants of staphylococcal nuclease (SNase) were used to characterize the diverse types of structural reorganization that can be promoted by the ionization of buried groups. NMR relaxation dispersion and ZZ-exchange experiments were used to identify the locations and measure the time scales and extent of pH-dependent conformational exchange in these two proteins. The buried Lys-25 and Lys-125 residues titrate with pK_a of 6.3 and 6.2, respectively. The L25K protein fluctuates between the native state and an ensemble of locally unfolded states on the 400 μ s to 7 ms time scale. On the 100 to 500 ms time scale the native state exchanges with a subglobally unfolded state in which the β -barrel is partially reorganized. The equilibrium between the native state and this alternative state is highly pH dependent; at pH values below the pK_a of Lys-25 the state with the partially reorganized β -barrel is the dominant state. In contrast, the L125K protein only exhibited pH-independent fluctuation in the microsecond to millisecond time scale in the region near Lys-125. The study illustrates how diverse and how localized the coupling between conformational reorganization and ionization of buried groups can be. The pH-sensitive exchange between the fully native and subglobally or locally unfolded states in time scales well into hundreds of milliseconds will challenge all computational methods for structure-based calculations of pK_a values.

Ionizable residues buried in the hydrophobic interior of proteins are of special interest owing to their anomalous ionization equilibria and to their essential roles in biological energy transduction^{1–3} and catalysis.^{4,5} Because the protein interior is less polarizable than water, buried ionizable groups usually have pK_a values very different from those of ionizable groups in water.⁶ To understand the structural basis of biological energy transduction, it is necessary to understand the structural and physical factors that determine these anomalous properties of buried groups, and the range of conformational transitions that can be promoted by their ionization. Those are two goals of this study.

The properties of buried ionizable groups in the energy transducing machines (e.g., ATPase or cytochrome c oxidase) that require buried ionizable groups for functional purposes cannot be examined experimentally. The NMR spectroscopy or

equilibrium thermodynamic experiments used to measure pK_a values^{7,8} cannot be applied systematically to these large, multisubunit integral membrane proteins. Structure-based pK_a calculations could be used instead to examine properties of buried ionizable groups and how ionization events are involved in mechanisms of energy transduction, but the accuracy of these calculations for the cases of buried ionizable groups is limited despite claims to the contrary.⁹ The problem with structure-based calculations is that proteins can respond to the ionization of buried groups with changes in structure or dynamics or both, and this is not reproduced well in these calculations.^{7,10–12} Here we have used staphylococcal nuclease

Received: May 13, 2015

Revised: September 2, 2015

Published: September 3, 2015



(SNase) as a model system to examine in detail the time scales and the nature of the structural reorganization coupled to the ionization of buried groups in proteins. Not only does this level of insight contribute general mechanistic understanding of the structural basis of energy transduction, it is necessary to guide improvements to structure-based energy calculations with proteins.

Use of SNase as a model system is justified by the unprecedented level of detail achieved with the NMR spectroscopy experiments that were used to examine the conformational response of SNase to the ionization of a buried Lys residue. The L25K and the L125K variants of SNase were used to characterize in detail the structural reorganization triggered both by the L25K and L125K substitutions and by the ionization of the internal Lys-25 and Lys-125. These two buried Lys residues were selected based on a previous study from this laboratory that examined qualitatively the consequences that the charging of buried Lys residues can have on the conformation and dynamics of SNase.¹³ This involved detection of resonance broadening and chemical shift changes in ¹H–¹⁵N HSQC spectra collected as a function of pH with 25 variants of SNase with internal Lys residues.¹³ The subset of proteins identified as undergoing conformational reorganization (L25K, F34K, V39K, V66K, L125K) on microsecond to millisecond time scales is of particular interest precisely because of the challenge they pose for structure-based pK_a calculations as well as for the insight they contribute toward mechanisms of biological energy transduction.^{14–16}

Three other variants of SNase with internal Lys residues with anomalous pK_a values were identified previously as exhibiting microsecond to millisecond time scale fluctuations: V66K, V39K, and F34K. These could also have shed light on structural responses to charging processes, but they were not used in this study for different reasons. The V66K variant has already been studied.⁷ The V39K variant was not chosen because the apparent pK_a of Lys-39 is 9, making NMR studies difficult owing to base-catalyzed hydrogen exchange. The F34K variant ($\Delta G^{\circ}_{\text{H}_2\text{O}} = 5.2$ kcal/mol at pH 8.0 and 3.8 kcal/mol at pH 6.0), the only other variant from the set that exhibited broadening concomitant with ionization of the internal Lys-34 (apparent pK_a = 7.1), revealed no microsecond to millisecond time scale dynamics upon further resonance assignment and screening by relaxation dispersion and ZZ-exchange experiments.

Owing to fluctuations of the backbone a buried ionizable group can experience different microenvironments with different electrostatic properties. The observed or apparent pK_a values that are measured experimentally actually represent an average of the pK_a values experienced by the ionizable groups in the different conformational microstates.¹⁷ One reason it is difficult to reproduce pK_a values of buried groups computationally is that the simulation of conformational changes that take place over time scales relevant to thermodynamic processes, which tend to be slower than microsecond, is very challenging.^{18,19} An important step toward the improvement of the accuracy of structure-based electrostatics calculations is to describe in detail the nature of the coupling between the ionization of buried Lys residues and the conformational state of the protein.

Comparative investigation of the L25K and L125K proteins highlights not only the heterogeneity of dielectric responses across different regions of the same protein, but also the challenge of understanding relationships between thermody-

namic stability, conformational reorganization, and the anomalous pK_a values of buried groups. The thermodynamic stabilities ($\Delta G^{\circ}_{\text{H}_2\text{O}}$) of both the L25K (4.6 kcal/mol at pH 7.5 and 2.7 kcal/mol at pH 5.5) and L125K (4.2 kcal/mol at pH 7.0 and 2.5 kcal/mol at pH 4.9) variants⁸ are lower than the stability of ~11.7 kcal/mol of the parent protein²⁰ throughout that entire pH range studied. The stability of the variants with the internal Lys is also highly pH-dependent in a way that the parent protein is not. Lys-25 and Lys-125 titrate with apparent pK_a values of 6.3 and 6.2, respectively. Although the pK_a values are similar, the internal Lys residues are located in very different parts of the protein and in very different microenvironments: Lys-25 is on strand 2 in the β -barrel and Lys-125 is on helix 3 on the other side of the protein (Figure 1).

The present study of the L25K and L125K variants of SNase involved the assignment of ¹H/¹⁵N resonances to identify the regions that underwent structural reorganization, and measurement of changes in chemical shifts, of relative resonance

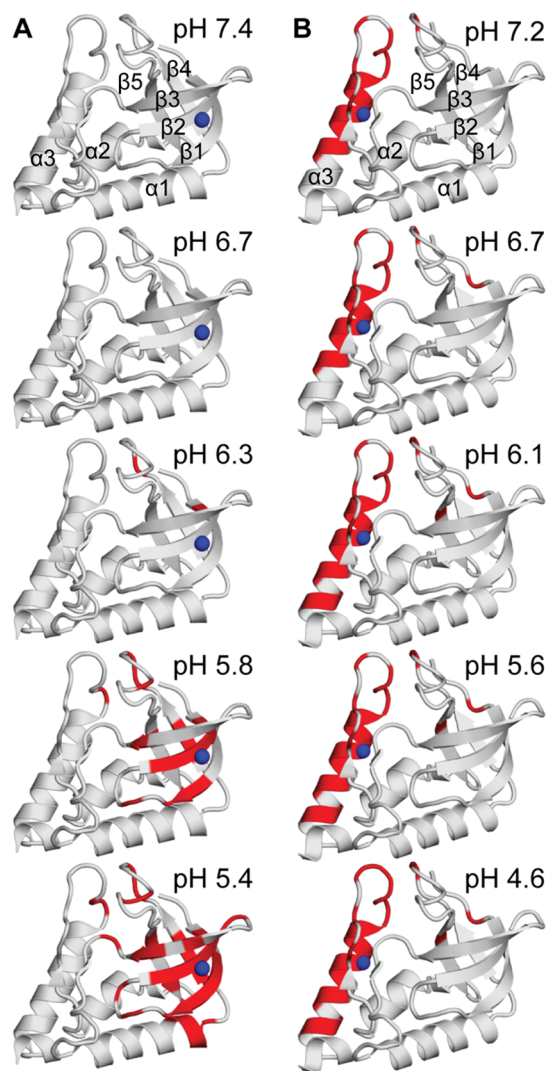


Figure 1. Residues shown in red are those for which resonances are broadened beyond detection in HSQC spectra measured at the indicated pH values. The structures shown are the actual structures of the (A) L25K variant (PDB ID: 3ERQ) and of the (B) L125K (PDB ID: 3C1E) variant.¹³ The locations of Lys-25 (pK_a = 6.3) and Lys-125 (pK_a = 6.2) in each protein are marked with a blue sphere.

intensities, and ^{15}N relaxation dispersion to determine the location and pH dependence of conformational reorganization. ^{15}N relaxation dispersion (RD) and ZZ-exchange spectroscopies were used to establish constraints on the time scales of fluctuation between conformations. RD experiments are useful to examine the microsecond to millisecond time scale because they reveal and quantify the relaxation of transverse magnetization caused by fluctuations in this time scale. In contrast, the ZZ-exchange experiments measure very slow fluctuations (>ms) by recording the two potentially different chemical shifts reported by a nucleus that samples two different conformations (the interconversion is sampled while the ^{15}N magnetization is in the “Z” orientation). In the L25K protein the ZZ-exchange experiments were also used to assign peaks for an alternative state and quantify rates of conformational reorganization.

Both the time scale and the nature of the conformational reorganization coupled to protonation of two buried Lys residues are described by the present study. The conformational transitions are described with the atomic resolution afforded by NMR spectroscopy. These data contribute stringent and exquisitely detailed benchmarks useful to determine if structure-based pK_a calculations and simulations of structural transitions coupled to the ionization of buried groups are accurate or even reasonable and relevant.^{9,21} The detailed description of the coupling between protonation and conformational equilibria achieved in this study is unprecedented and beyond what can be achieved with constant pH molecular dynamics simulations.⁹

MATERIALS AND METHODS

Protein. ^{15}N -labeled samples were used for purposes of assignment for the L25K protein, and for assignments, relaxation dispersion, and ZZ-exchange data for the L125K protein. They were prepared as described previously.¹³ For collection of relaxation dispersion, ZZ-exchange, and pH dependence data for the L25K variant, ^2H , ^{15}N -labeled samples were also purified as described previously except that bacterial growth was begun in LB media followed with resuspension and growth in D_2O minimal media for 1 h, one 4-h period of induction with 1 M IPTG, followed by a 2-h period of induction with an additional 1 M IPTG.

Resonance Assignment. Standard HNCACB, CBCACONH, and HSQC spectra were collected at pH 6.7 for the L25K protein and pH 7.2 for the L125K protein. Sparky was used to assign the HSQC spectra.²² Sparky was used to transfer assignments throughout HSQC and TROSY titration experiments.

NMR Relaxation Dispersion Spectroscopy (RD). NMR spectroscopy experiments were performed at 298 K on 600 MHz Bruker Avance II (for L25K) and Avance (for L125K) spectrometers with cryoprobes and on an 800 MHz Varian INOVA spectrometer without cryoprobe. The improved ^{15}N CPMG single-quantum relaxation-compensated RD pulse sequence was used.²³ For the L25K protein, dispersion experiments were collected, at pH 6.3, by varying the repetition of CPMG elements in a constant-time R_2 relaxation period (28.8 ms); 10 different ν_{CPMG} ($= 1/4\tau_{\text{CPMG}}$) values and two duplicates were collected at each static magnetic field strength: At 600 MHz the ν_{CPMG} values were 34.92, 70.22, 105.93 ($\times 2$), 142.05, 178.57, 367.65, 568.18 ($\times 2$), 781.25, and 1008.06 Hz. At 800 MHz the ν_{CPMG} values were 34.97, 70.42, 142.86 ($\times 2$), 217.39, 373.13, 538.44, 714.29 ($\times 2$), 853.53, and 1000.00 Hz.

Spectra were collected with interleaved data collection over approximately 80 h.

R_2 vs ν_{CPMG} dispersion series from the L25K protein were fit to two-site exchange models using the RD module of the program RELAX.²⁴ Parameter errors were calculated by RELAX and are the standard deviations of 500 Monte Carlo simulations constrained by the input data. Model selection was performed according to the Akaike Information Criterion. RD time series were best fit with one of two two-state exchange models: the reduced Carver-Richards equation (CR72, in the nomenclature of the relax software), for which the parameters k_{ex} , P_A , and $\Delta\omega_N$ are calculated;²⁵ or the analytical expression for very slow exchange by Tollinger et al. (TSMFK01), which yields the parameters k_{AB} and $\Delta\omega_N$.

For estimates of R_{ex} and exchange regime in both the L25K and L125K variants two ν_{CPMG} values at two static field strengths were used: 34.92 and 1008.06 at 600 MHz, 34.97 and 1000.00 at 800 MHz. For the L25K protein this was done at pH 6.3. For the L125K protein this was done at both pH 7.2 and 5.2. Estimates of R_{ex} were calculated with the equation $R_{\text{ex}} = \ln(I_{\text{few}}/I_{\text{many}})/T$ where I_{few} and I_{many} are the peak intensities from the low and high CPMG frequency spectra, and T is the constant-time R_2 relaxation period length.

NMR Exchange Spectroscopy. 2D (H_2N), 2D (H_2H), and 3D ($\text{H}_2\text{H}_2\text{N}$) versions of a standard ^{15}N ZZ-exchange experiment²⁶ were used to locate cross-peaks and assign peaks corresponding to the alternative state of the L25K protein at pH 6.3. Mixing times were 0.2, 0.5, 1.2 s in the 2D spectra and 0.8 s in the 3D. For estimation of kinetic parameters in the L25K protein by ZZ-exchange, 2D (H_2N) spectra were collected with 10 mixing times, two repeated: 0.0237, 0.0567, 0.1007, 0.1557, 0.1997 ($\times 2$), 0.2987, 0.3977, 0.4967 ($\times 2$), 0.6507, 0.8487 s. Decay and build-up data were then modeled by least-squares fitting of the equations as in Farrow et al.²⁶ 2D (H_2N) and 2D (H_2H) ^{15}N ZZ-exchange spectra with mixing times 0.2, 0.6, and 1.0 s were used to screen for slow exchange in the L125K protein at pH 6.1.

pH Dependence of Populations in the L25K Protein. 2D H_2N TROSY spectra were collected at pH 5.3, 5.7, 6.3, 6.8, and 7.2. Native (“A”) state peak assignments were transferred from the HNCACB and CBCACONH assignment process described under Resonance assignment above, and peak assignments for the alternative (“B”) state were transferred from the ZZ-exchange spectrum assignments described above. At each pH value the B-state population fraction (P_B) or each residue was estimated using the expression $P_B = H_B / (H_A + H_B)$ where H_A and H_B are the heights of the A- and B-state peaks, respectively, for that residue.

Analytical and Visualization Tools. Analysis code (with the exception of Sparky and relax as referenced above) was built with IPython,²⁷ pandas,²⁸ NumPy,²⁹ Matplotlib,³⁰ seaborn (<http://stanford.edu/~mwaskom/software/seaborn/>) and LMFIT (<http://lmfit.github.io/lmfit-py/>) and is available in an IPython Notebook at <http://github.com/drichman/protein-nmr-analysis/notebooks> and also available from the authors upon request.

RESULTS

L25K Variant: Assignment and pH Dependence of Broadened Resonances. Spectra of the L25K protein could be completely assigned (to the extent that the parent protein could be assigned) at pH conditions above (pH 7.4 and 6.7) and at the pH corresponding to the pK_a of 6.3 for Lys-25

(Figure 1A and Table S1). Most of the HSQC spectra remained unaffected by the titration of Lys-25, indicating that structural reorganization was local. An extensive loss of peaks assigned to the β -barrel residues was observed at pH values immediately below (pH 5.8) the pK_a ; the number of severely broadened peaks increased as the pH decreased further to pH 5.4. This type of broadening, and its localization on the structure, is consistent with conformational exchange, on the microsecond to millisecond time scale, of the β -barrel backbone. The locations that were affected or their exchange regime show pronounced pH dependence (Figure 1A).

L25K Variant: Locations of Conformational Exchange and Time Scales Characterized by Backbone ^{15}N Relaxation Dispersion. At pH 6.3, which corresponds to the apparent pK_a of Lys-25, many resonances from residues comprising and neighboring the β barrel exhibited RD consistent with the presence of two disparate exchange processes, one occurring between hundreds of microseconds and several milliseconds, and the other occurring in hundreds of milliseconds (Figure 2A and Table S2). Most reporters of RD were characterized by large R_{ex} values that varied significantly between static field conditions (Figure S1), which, following in the interpretation of Millet et al. and Tollinger et al.,^{31,32} indicates the presence of faster exchange

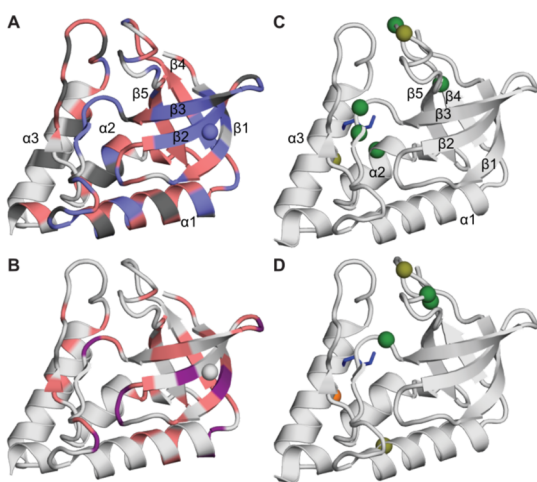


Figure 2. Locations that experience fluctuations in the microsecond to millisecond time scale according to relaxation dispersion (RD) and ZZ-exchange experiments (slow-exchange spectroscopy). (A) Results from RD analysis of the L25K protein at pH 6.3. Sites with 0.4–7 ms (blue) or 10–500 ms (pink) exchange rates identify the backbone amides that experience chemical exchange in the μs –ms time scale (i.e., a significant R_{ex} component to transverse relaxation). Amides with no R_{ex} are shown in light gray. Amides for which there are no data are shown in dark gray. (B) Residues for which resonances from both conformational states A and B were detectable at pH 6.3 (pink), and residues used to quantify the exchange rates through ZZ-exchange spectroscopy (purple). (C, D) Results with the L125 K protein at two pH values. The structure shows the locations that experience significant fluctuations in the microsecond to millisecond time scale. The color indicates the estimates of the exchange regime calculated from R_{ex} estimates at two static magnetic fields (14.1 and 18.8 T). Amides in the slow regime ($k_{ex} < \Delta\omega_N$, the chemical shift difference between states) are shown as orange spheres. Amides in the intermediate regime ($k_{ex} \approx \Delta\omega_N$) are shown as light green spheres. Amides in the fast regime ($k_{ex} > \Delta\omega_N$) are shown as dark green spheres. The side chain of the internal Lys-125 is shown in stick representation in blue.

processes. Yet unlike the system studied by Tollinger et al., in which the folded state exchanged slowly with an unfolded state, which then experienced relatively fast interconversions among different unfolded states, in the L25K variant of SNase the native state resonances report the two different exchange regimes. The native state interconverts with two different sets of locally or subglobally unfolded states, each separated in time scale by hundreds of milliseconds. Even though these reorganization processes involved transitions to ensembles of partially or locally unfolded conformations, they were modeled as two-state exchange processes. Two-state exchange is the simplest model that approximates the conformational reorganization of the L25K protein because the partially or locally unfolded ensembles can still be represented on average as the alternative (“B”) state.

Exchange rates (k_{ex}) in the faster regime ranged from approximately 130 s^{-1} to 2500 s^{-1} , with an average of $\sim 650\text{ s}^{-1}$ (Table S2 and Figure S2A). This range of rates corresponds to motional time scales between about 0.4 and 7 ms, with most residues fluctuating in the millisecond time scale. High error in parameter estimates is probably a result of inadequacies of the models used for analysis and error in the R_2 measurements ($\pm 3\text{ s}^{-1}$). Models built for situations of high population imbalance ($P_B < 0.1$) were applied to some residues that exhibited $P_B \approx 0.3$ or 0.4 , as measured from peak heights; B-state population fractions of ~ 0.1 cause $\sim 12\%$ errors in parameter estimates.³³ Residues fit to the slower regime report forward exchange rates (k_{AB}) between approximately 1 and 20 s^{-1} (Table S2 and Figure S3A). Since k_{ex} is the sum of forward (k_{AB}) and backward (k_{BA}) rates it can be derived from $k_{ex} = k_{AB}/P_B$. With population fractions of the partially unfolded forms at pH 6.3 of ~ 0.2 or 0.7 (for different parts of the structure), as will be described below, the very slow process detected through RD corresponds with k_{ex} values between ~ 2 and 80 s^{-1} , or time scales of tens of milliseconds to 500 ms.

L25K Variant: Locations of Conformational Exchange and Time Scales Characterized by Backbone ^{15}N ZZ-Exchange. Many peaks belonging to the average alternative state (referred to as the B-state) could be resolved in an (H,N)-TROSY spectrum of the L25K protein at pH 6.3 and assigned using multidimensional ZZ-exchange spectra. Several other residues appeared to produce cross-peaks in ^{15}N ZZ-exchange spectra that were recorded as (H,H) or (H,H,N) correlations for more resolved readout, but corresponding resonances in the B state could not be found, possibly due to overlaps or lack of resolution in the crowded unfolded band of (H,N) spectra. Nonetheless, the detection of cross-peaks in ZZ-exchange spectra recorded with mixing times on the order of hundreds of milliseconds corroborates the presence of the very slow exchange process indicated by analysis of RD data. The residues with assignable A and B peaks are shown in Figure 2B, and they can be compared with the locations of fluctuation reported by RD analysis (Figure 2A).

Forward and reverse exchange rates (k_{AB} and k_{BA}) were estimated through the formalism defined in Farrow et al.²⁶ for a subset of residues for which all A- and B-state peaks and interconversion cross-peaks could be clearly assigned in H,N-correlated ZZ-exchange spectra. The total exchange rates, or $k_{ex} = k_{AB} + k_{BA}$, for β -strand residues Thr-13, Leu-14, Gly-20, Asp-21, and Leu-24 were between 1 and 2.5 s^{-1} . The forward rates were ~ 2 times higher than the reverse rates. The total exchange rates for Gly-29, Leu-38, Phe-50, Asn-68, and Ala-69, which are mostly loop and helix residues, ranged between 3 and 22 s^{-1}

and had forward rates 2–4 times lower than reverse rates (except Gly-29, which had poor fit quality) (rates listed in Table S3, decay and build-up curves and fits shown in Figure S4). These are consistent with the rates reported as the slower of the two time scales in the RD analysis. They corroborate the presence of a very slow exchange process in the hundreds of milliseconds.

L25K Variant: Chemical Shifts of the Alternative State.

Considered as a set, the resonances from the B conformation show less dispersion of ^1H chemical shifts than resonances from the A state (Figure 3 and Table S4). The decrease in dispersion

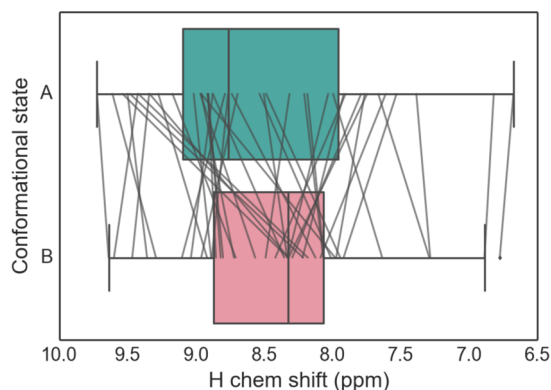


Figure 3. Box and whisker plot showing distributions of ^1H chemical shifts for resonances belonging either to the “A” state (green) or to the “B” state (pink). Left and right box borders reflect the interquartile range (IQR) between the 25% and 75% quartiles; the inner line denotes the median. Whiskers mark values 1.5 times beyond IQR bounds.

is consistent with loss of native structure,^{34,35} particularly at and near the β -barrel. However, the loss of dispersion is not significant enough to imply that a completely unfolded, near random-coil conformation is being populated in state B. Furthermore, because chemical shifts of B-state peaks had negligible pH dependence (Figure S5A), the exchange was assumed to be within the very slow regime, and peak positions represent almost completely the alternative states rather than a population-weighted average.

^{15}N chemical shift differences ($\Delta\omega_{\text{N}}$) derived from the spectrum at pH 6.3 were compared to those derived from RD model fitting at pH 6.3; the exact correlation was poor: model fitting did not strictly reproduce the values measured in the spectrum. However, fitting did capture the overall trend: the calculated $\Delta\omega_{\text{N}}$ values were appropriately small for most residues with small measured $\Delta\omega_{\text{N}}$, and appropriately large for residues with large measured $\Delta\omega_{\text{N}}$ (Figure S5B).

L25K Variant: pH Dependence of Population Distribution. The population of conformational state B increases from the 0.01–0.2 range at pH 7.2, where Lys-25 is neutral, to the 0.2–1.0 range below pH 5.8, where it is charged (Figure 4). These distributions were derived from native and alternative peak heights from residues around or neighboring the β barrel. The strongly pH-coupled population shifts are roughly organized into groups: β -strands 1 and 2 exhibit the strongest pH dependence, their B-state populations rising from between 10 and 20% to almost 100% as pH drops from 7.2 to 5.3 (labeled in red in Figure 4). By comparison there is a group of “medium” pH dependence (shown in green in Figure 4) and one of “low” pH dependence (shown in blue in Figure 4), and

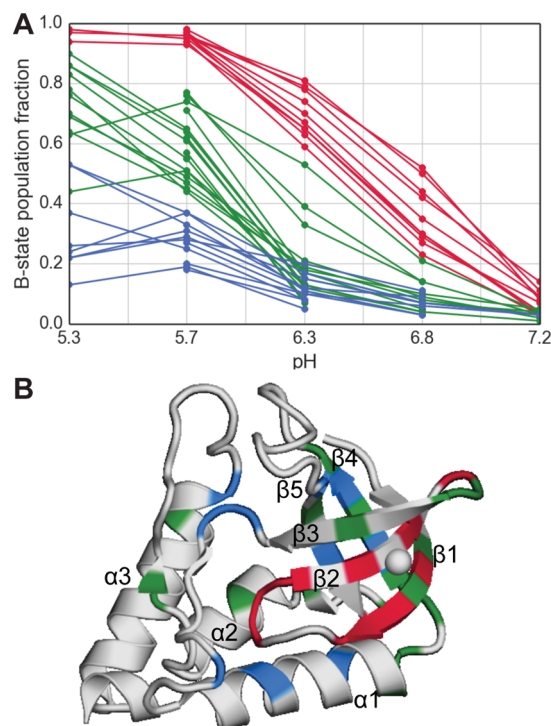


Figure 4. (A) Population fraction of conformational ensemble B of the L25K protein as a function of pH. These population fractions were derived from peak heights. (B) Locations corresponding to the residues tracked in (A).

those residues are more randomly distributed in the structure, but they do still imply subglobal structural reorganization centered at the β barrel. The “medium” pH dependence B-state reporters show a population increase from less than 10% at pH 7.2, to 40–90% at pH 5.7 and 5.3. This largely describes β strands 4 and 5, although three of these reporters are actually outside the β barrel, one each in helices 2 and 3 and one in the loop preceding helix 3. The “low” pH dependence B-state reporters show a population increase from less than 10% at pH 7.2 to 20–40% at pH 5.7 and 5.3. These reporters are also found in β strands 4 and 5, in addition to helix 1 (which forms the bottom cap of the β barrel) and loops adjacent to the barrel.

Compared to the alternative-state population fractions derived at pH 6.3, RD model fitting consistently underestimated population fractions above ~ 0.1 (Figure S5C), which is expected given the nature of the RD models and their underlying assumptions of small alternative-state populations.

L25K Variant: Assignment and pH Dependence of Broadened Resonances. All residues except Lys-125 and approximately four contiguous neighbors on either side of 125 in the sequence, and several in the preceding loop, could be assigned at all measured pH conditions (7.2, 6.7, 6.1, 5.6, 4.6) (Figure 1B and Table S2). This pattern of broadened resonances for Lys-125 and its neighbors is consistent with conformational exchange in the microsecond to millisecond time scale. The data did not allow any possible inference of pH dependence in the pattern of broadening. We infer that the amides of the segment in question are reporting backbone conformational reorganization rather than reporting chemical exchange from motion of the Lys side chain because the charge state of the Lys side chain seems to have no effect on the broadening.

L125K Variant: Locations of Conformational Exchange and Time Scales Characterized by Backbone ^{15}N Relaxation Dispersion. Because resonances from residues in the top half of helix-3 were missing at all pH conditions, RD measurements were made using detectable resonances elsewhere in the protein to constrain the exchange time scale and to check further for pH dependence. At pH conditions above and below the pK_a of 6.2 of Lys-125, significant R_{ex} values were estimated for several locations (disregarding the protein's overall N and C termini), especially at residues 37–39, found in apposition with Lys-125 on an occluding loop, and at several residues of strand $\beta 5$ that are part of the contacts or interactions between helix-3 and the β barrel (Figure S6).

Sets of residues that are slightly different from each other (but mostly neighbor each other) report significant R_{ex} values at pH 5.2 compared to pH 7.2, with a few residues reporting R_{ex} under both conditions. Overall, the R_{ex} magnitudes were 2–3 times higher at pH 7.2, where Lys-125 is only 10% ionized, than at pH 5.2, where it is 90% ionized. This is counterintuitive. However, reporters of R_{ex} indicate that exchange occurs in the fast regime at both pH conditions based on the exchange parameter α derived from comparison of R_{ex} values estimated at static magnetic fields of 14.1 and 18.8 T (Figure 2C,D and Table S5).³¹ The R_{ex} estimates also support the conclusion that there is no strong pH dependence, as inferred from the pattern of broadened peaks throughout the titration.

L125K Variant: Absence of ZZ-Exchange Cross-Peaks. Although a small number of extra peaks were present in the spectra of the L125 K protein, ZZ-exchange experiments failed to reveal any cross-peaks. Lack of exchange cross-peaks is consistent with conformational exchange in the microsecond time scale but not in the millisecond time scale, and consistent with the above estimate from R_{ex} measurements that the exchange regime is fast. The few extra peaks could originate from alternative form in extremely slow exchange (>seconds).

DISCUSSION

The experiments with the L25K and L125K variants of SNase revealed structural details, time scales, and pH dependence of conformational reorganization coupled to the ionization of single Lys residues buried in the hydrophobic cores of the protein. These two variants were engineered in the highly stable $\Delta\text{+PHS}$ variant of SNase.⁸ They were selected from the set of SNase variants with internal Lys residues on the basis of their having anomalous pK_a values and qualitative evidence of conformational reorganization coupled to the ionization of the buried Lys.¹³ Lys-25 in the L25K variant titrates with an apparent pK_a of 6.3 and Lys-125 in the L125K variant titrates with an apparent pK_a of 6.2.

It is known that the titration of the internal Lys residues does not affect the titration properties of the other groups that titrate in the range of pH between 5 and 9.⁸ This is evident from the pH dependence of stability measured by chemical denaturation, which can be explained exactly by the shift in the pK_a of the buried Lys. There are only three residues that titrate in this range of pH: (1) His-8 ($\text{pK}_a = 6.5$), which in the N-terminus of the protein and is known to be disorganized;³⁶ (2) His-121 ($\text{pK}_a = 5.25$), which is at the N-terminus of helix 3 and makes H-bond contacts at the interface of the protein;³⁷ and (3) Asp-21 ($\text{pK}_a = 6.5$), which interacts with neighboring carboxylic groups in the active site.³⁸ In the background protein the titrations of His-8, His-121, and Asp-21 are coupled to local

fluctuations characterized by small amplitude and high frequency. They are not involved in the more pronounced unfolding events observed in the L25K and L125K variants.³⁹

As is the case with all internal ionizable groups, it is never obvious what determines the anomalous pK_a values of Lys-25 and Lys-125. The general direction of the shift reflects the difference between the dielectric effect of water and that of the protein interior. What the NMR experiments with these two proteins make abundantly clear is that the actual magnitude of the shift in pK_a relative to the normal pK_a value of 10.4 for Lys in water has less to do with the polarity and polarizability of the microenvironments and more with the probability of conformational reorganization coupled to the ionization of the buried Lys.

A survey of the variants of SNase with internal Lys residues, performed by inspection of ^1H – ^{15}N HSQC spectra measured over the pH range around the pK_a revealed that the L25K and L125K proteins exhibit pH-dependent conformational reorganization. The similarity in their pK_a values despite differences in their location (Lys-25 is on strand 2 in the β barrel and Lys-125 is on helix 3 on the other side of the protein) suggested that a comparison of the two variants would contribute physical insight into structural and dynamic consequences of ionization of a Lys residue in hydrophobic environments. The insight is necessary to guide modifications to methods for structure-based analysis of electrostatic effects. The data that emerge from these studies constitute stringent benchmarks useful for the critical evaluation of the performance and accuracy of computational models of protein electrostatics in terms of their ability to identify or reproduce the locations, time scales, and pH dependence of conformational reorganization.

Time Scale of Events. The L25K and L125K proteins undergo conformational reorganization in the microsecond to millisecond time scales. The L25K protein displays conformational reorganization on two different time scales, between 400 μs and approximately 7 ms, and between approximately 100 and 500 ms. Many of the residues that report a hundreds-of-microseconds process are the same residues that can populate alternative conformations (an average “B-state”), which was more related to processes occurring in the hundreds-of-milliseconds. The two time scales are reconcilable: residue-by-residue variability of the exchange rates and the pH-driven population shifts is consistent with reorganization processes involving two ensembles of non-native states.

The two ensembles are characterized by varying degrees of unfolding or reorganization. In the faster time scale (hundreds of microseconds), immediate neighbors in sequence display widely different exchange rates. This is consistent with an ensemble of states, each characterized by short (say 1–3 residue) segments in non-native conformations (this can be thought of as local unfolding). The slower time scale (hundreds of milliseconds), in which alternative-state chemical shifts and peak heights can be directly measured, consists of an ensemble of states in which entire β strands or sets of strands unfold in concerted ways (subglobal unfolding). Several tens or hundreds of the local unfolding fluctuations can take place between or during the subglobal unfolding events, which take place in hundreds of milliseconds. In other words the conformational energy landscape can be pictured as being comprised of (1) a native state, (2) a large ensemble of many locally unfolded states that are accessed in the hundreds of microseconds to a few milliseconds, (3) an ensemble of states with a substantially reorganized or partially unfolded β barrel (the subglobally

unfolded state ensemble, accessed in the hundreds of milliseconds), and (4) a fully unfolded state or ensemble of states.

The native state is usually assumed to refer to the completely folded state represented by the crystallographic structure. Measurements of thermodynamic stability ($\Delta G^\circ_{\text{H}_2\text{O}}$) with equilibrium experiments based on Trp fluorescence as a reporter of the native state report on this fully folded native state but also on the many locally unfolded conformations interconverting on hundreds-of-microseconds time scales that were observed in the NMR spectroscopy experiments. The $\Delta G^\circ_{\text{H}_2\text{O}}$ derived from Trp fluorescence can reflect the presence of states with free energies that lie between the fully unfolded and fully native state energies, resulting in a smaller measured $\Delta G^\circ_{\text{H}_2\text{O}}$ than the $\Delta G^\circ_{\text{H}_2\text{O}}$ that truly represents difference in free energy between the fully folded and the fully unfolded states. A state that is non-native that does not perturb the local environment of Trp-140 in SNase would have the same spectroscopic signature as the fully native state; for example, states with a native and partially unfolded β barrel both have the possibility of leaving helix 3 and Trp-140 unperturbed.

For the L125K protein, the lack of crosspeaks in ZZ-exchange spectra was interpreted as suggesting that the reorganization time scale is restricted to hundreds of microseconds and does not include any events in the milliseconds. RD indicated that several residues undergo fast exchange, implying small $\Delta\omega$, large k_{ex} or both. The ZZ-exchange and RD observations support the conclusion that the dominant mode of conformational reorganization in the L125K protein takes place on a faster time scale than reorganization in the L25K protein. By comparison to the time scales detected for the L25K protein, we inferred that the maximum time scale of reorganization (most likely the loss of helical structure) of helix-3 in the L125K protein (the segment whose resonances are broadened) is in the low hundreds of microseconds.

The enhanced conformational sampling in constant-pH MD simulations (CpHMD) precludes exact interpretation of the time scales of the simulations as physical time scales. Nonetheless it seems unlikely that even the inferred physical time scales of simulations such as those by Shi et al.⁹ and Goh et al.²¹ are in the same order of magnitude as the reorganization events measured here. The extensive structural change observed, such as segmental unfolding, and the relatively long time scales over which it occurs, exceed the capabilities of most classical MD simulations, but they are within striking range of the time scales that can be examined with Anton simulations.⁴⁰ The data from our NMR spectroscopy studies offer an excellent opportunity for testing the ability of MD simulations to reproduce ligand driven conformational transitions (H^+ being the simplest and smallest ligand possible). According to our results, the problem of pK_a calculations for the case of buried groups in proteins involves predicting alternative states of proteins and calculating the energy differences and probabilities of the different states over a range of pH as well as the relevant time scales. This will require exquisitely accurate force fields that can capture accurately the difference in the self-energy of a charged species in water and in the complex dielectric environment inside the protein.

The results of Shi et al.⁹ and Goh et al.²¹ suggest that conformational reorganization in some variants of SNase with internal Lys residues can be observed within nanoseconds of simulations. In this time scale a few water molecules penetrate

the protein and approach the charged moiety of the internal Lys residue. Their results suggest that this type of structural relaxation is sufficient to account for a microstate in which the pK_a of the internal Lys is normal. If all that were detected experimentally were motions in the time scale of nanoseconds (or even low-microseconds) it would be possible to conclude that the pK_a values of internal Lys residues are determined by dynamic events in fast time scales and by the transient presence of partially unfolded states. But the situation appears to be more complicated and more interesting because microsecond to millisecond motions are detected in our NMR spectroscopy experiments. These are long time scales that begin to overlap with those relevant to the equilibrium thermodynamic experiments used to measure pK_a values experimentally. At least for these internal Lys residues in SNase, and possibly for other Lys residues for SNase and for other buried ionizable groups in proteins, conformational reorganization in the μs -ms time scales is reflected in the pK_a values. Accurate sampling of reorganizational processes in these time scales should increase the accuracy of structure-based pK_a calculations for cases of buried groups.

Identity of an Alternative State. Besides demonstrating that the proton binding-coupled conformational reorganization of the L25K variant of SNase happens in a long time scale, this study shows that locally or subglobally unfolded or reorganized conformations are sampled and that this governs the properties of Lys-25. On the basis of the location of slow and very slow exchange, on the variety of rates, and on dispersion of chemical shifts, it is possible to infer that in response to the ionization of Lys-25 the protein reorganizes into an ensemble of locally and subglobally partially unfolded forms. The locations of residues in the L25K protein that can be assigned to alternative-state resonances, which describe the longest-time scale reorganization phenomena in the set of observations, are distributed in nonuniform ways in some parts of the protein, and in clusters of consecutive residues in others. The latter are consistent with what would be expected for a concerted transition to a distinct state. Similarly, some residues report exchange rates of different orders of magnitude from their neighbors. These observations are consistent with a rugged landscape of conformational states in which a residue may be a member of certain conformational excursions and not others, different even from a neighbor. The alternative-state ^1H chemical shift distribution, which is decreased compared to a native-like distribution but not completely collapsed, further supports interpreting what was detected as an ensemble of alternative states, all of which are native-like except for having one or another part of the β barrel in a non-native conformation. This kind of diversity of possible conformational states represents a challenge to simulations and rules out the utility of techniques that use *a priori* knowledge of states, such as umbrella sampling.

In contrast to the behavior of the L25K protein, the conformational reorganization of the L125K protein induced by the presence and ionization of Lys-125 occurs on a faster time scale and affects a smaller number of residues, but it too is most consistent with partial unfolding rather than a concerted response. Acid unfolding of this protein, monitored by circular dichroism spectroscopy at 222 nm showed a decrease in the predenaturation baseline amplitude with decreasing pH that was more severe than for many other variants.⁸ This could be interpreted as a loss of helical structure coupled with the titration of Lys-125.⁸ In general our findings are somewhat at odds with the simulation by Goh et al. that reports very slight

rearrangement of the fully folded structure of the L125K protein upon ionization of Lys-125. But considering the time scale of the conformational effects we observe as well as the considerations of local stability and cooperativity described above, it is not unexpected for existing force fields and sampling methods to be limited in their ability to reproduce the complex conformational reorganization and subglobal unfolding reported by the NMR spectroscopy experiments.

pH Dependence of Conformational Equilibria. The conformational reorganization in the L25K and L125K proteins differs most notably in how it is affected by changes in pH. Residues in and near the β barrel show that decreasing pH increases the fraction of the alternative state in the L25K protein. Observation of this type of proton binding-coupled conformational reorganization was anticipated for proteins with internal ionizable residues (Figure 5), but the dramatic example

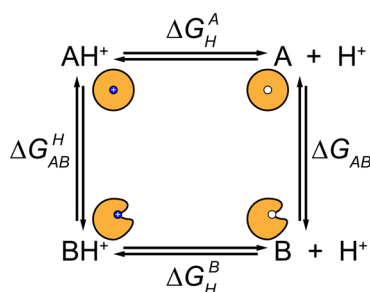


Figure 5. Coupling of proton-binding equilibria and conformational equilibria between states A and B. Simulations of the experimental data suggest that in the L125 K protein $\Delta G_{AB} = 1.5$ kcal/mol (i.e., energy of the conformational reorganization A to B when Lys-125 is neutral), $pK_a^A = 4$ (deprotonation of Lys-125 in the A state), and $pK_a^B = 8.5$ (deprotonation of Lys-125 in the B state).

provided by the L25K protein is especially striking in contrast with the relative pH-independence of conformational exchange in the L125K protein. In the case of the L25K protein the native β -barrel fold is sufficiently stable to require a substantial degree of proton binding to the internal Lys to promote occupancy of the reorganized or partially unfolded state in which the β -barrel is disrupted. In contrast, in the L125K protein the structure of the protein readily reorganizes in the vicinity of Lys-125 even when the fraction of charged Lys-125 remains small. The response to the ionization of the internal Lys in these two proteins is very different, yet the nearly identical apparent pK_a values and the global thermodynamic stabilities ($\Delta G_{H_2O}^\circ$) that are both pH dependent to nearly the same extent ($\Delta G_{H_2O}^\circ \approx 4.5$ kcal/mol when the internal Lys is neutral, ~ 2.5 kcal/mol when charged) mask these differences.

Earlier it was proposed that pK_a values measured experimentally represent weighted averages of the microscopic pK_a values experienced by an ionizable group in different structural microstates.¹⁷ A useful formalism to describe this through coupled proton binding and conformational exchange equilibria was proposed by Di Russo et al.,⁴¹ and this formalism has also been used by others^{9,21} (Table S7 and Figure S7). With this formalism the apparent pK_a values of 6.3 and 6.2 for Lys-25 and Lys-125, respectively, can be approximated using three parameters: (1) ΔG_{AB} (equilibrium between the deprotonated A and B states), (2) the Lys pK_a in the A state (pK_a^A), and (3) the Lys pK_a in the B state (pK_a^B). If A represents the fully native state and B an average of non-native or subglobally

unfolded states, then ΔG_{AB} must never be larger than $\Delta G_{H_2O}^\circ$, the global unfolding stability.

For the L25K protein, the simulations suggested that reasonable estimates for ΔG_{AB} are 2–4.5 kcal/mol, with pK_a^B between 8 and 10 and pK_a^A less than 5. Because the population of state A is dominant, pK_a^A does not have to be extremely shifted; at least 1 pH unit below the apparent pK_a of 6.3 is sufficient, but the actual value is not important. Rather, changing the energy gap between states A and B (ΔG_{AB}) and changing pK_a^B have the strongest effect on apparent pK_a . In other words the ability of the protein to populate states in which the pK_a value of the Lys is normal is the most important factor that determines the magnitude of the measured pK_a . This would be consistent with the existence of an ensemble of states in which even just one β -strand of the β barrel has been disrupted, sufficient to allow for hydration of the Lys residue and normalization of its pK_a .

For the L125K protein, the simulations suggested that the energy gap between A and B states was smaller than for the L25K protein. This was consistent with the observation that the B state of the L125K protein is more readily accessible at all pH, as inferred from pH-independent broadening in NMR spectra. Values of $\Delta G_{AB} = 1.7$ kcal/mol and $pK_a^B = 7.5$ yielded the apparent pK_a of 6.2 and an estimated B fraction of ~ 0.1 even at high pH. If the B state of the L125K protein consists of a perturbed helix 3, one would expect Trp-140 in that state to produce a different spectroscopic signature than in the fully native state. However, the Trp-fluorescence unfolding experiment could still obscure this intermediate state if the state is very close in energy to the fully native state, as we conclude it is here. The denaturation reaction previously observed by circular dichroism at 222 nm reported a slightly lower than normal native baseline that further decreased with pH, consistent with loss of some helical structure coupled with the titration of Lys-125.⁸ Observed by NMR spectroscopy, the exchange rates and chemical shift changes involved in this reorganization may evolve throughout the titration in such a way that the intermediate regime of NMR broadening obscures the underlying pH dependence of the coupled equilibria.

CONCLUSIONS

These studies show that the conformational reorganization that governs the magnitude of the pK_a values of buried Lys residues in SNase is complex and is itself governed by local stabilities and local structural properties. The results suggest that accurate calculation of some electrostatic effects in the proteins interior will require accurate sampling of conformational reorganization, prediction of alternative states, accurate calculation of free energy gaps, and handling of conformational changes in time scales that can be slower than milliseconds. We have described both the time scale and the nature of the conformational reorganization coupled to the ionization of two Lys residues in SNase with the high resolution afforded by NMR spectroscopy. These data constitute unprecedented, stringent benchmarks useful to examine the accuracy of structure-based pK_a calculations and simulations of structural transitions coupled to the ionization of buried groups.

■ ASSOCIATED CONTENT

■ Supporting Information

The Supporting Information is available free of charge on the ACS Publications website at DOI: 10.1021/acs.biochem.5b00522.

Table S1. L25K and L125 K residues missing due to broadening. Table S2. L25K RD model selection and parameter results. Table S3. L25K ZZ-exchange fitting parameter results. Table S4. L25K A/B-state chemical shift differences and peak heights. Table S5. L125 K exchange regime estimates. Figure S1. L25K R_{ex} estimates. Figure S2. L25K RD model CR72 fit results. Figure S3. L25K RD model TSMFK01 fit results. Figure S4. L25K ZZ-exchange decay and build-up fit results. Figure S5. L25K chem. shift difference vs pH and correlations between fitted and measured parameters. Table S6. Values for plot of L25K chem. shift differences vs pH. Figure S6. L125 K R_{ex} estimates. Table S7. Formalism for simulation of linked equilibria. Figure S7. Example plots of population fraction vs pH from simulation of linked equilibria (PDF)

■ AUTHOR INFORMATION

Corresponding Author

*E-mail: bertrand@jhu.edu. Phone: 410-516-4497. Fax: 410-516-4118.

Funding

This research was supported by NIH grant GM-061597 to B.G.-M.E.

Notes

The authors declare no competing financial interest.

■ ACKNOWLEDGMENTS

All data collected at the JHU Biomolecular NMR Center.

■ ABBREVIATIONS

SNase, staphylococcal nuclease; RD, relaxation dispersion; CR72, Carver-Richard 1972; TSMFK01, Tollinger, Skrynnikov, Mulder, Forman-Kay, Kay 2001; CpHMD, constant-pH molecular dynamics

■ REFERENCES

- (1) Luecke, H., Schobert, B., Richter, H.-T., Cartailler, J.-P., and Lanyi, J. K. (1999) Structure of bacteriorhodopsin at 1.55 Å resolution. *J. Mol. Biol.* 291, 899–911.
- (2) von Ballmoos, C., Wiedenmann, A., and Dimroth, P. (2009) Essentials for ATP Synthesis by F1F0 ATP Synthases. *Annu. Rev. Biochem.* 78, 649–672.
- (3) Gennis, R. B. in *Biophysical and Structural Aspects of Bioenergetics* (Wikström, M., Ed.) pp 1–25, Royal Society of Chemistry, Cambridge, 2005.
- (4) Ho, M.-C., Ménétret, J.-F., Tsuruta, H., and Allen, K. N. (2009) The origin of the electrostatic perturbation in acetoacetate decarboxylase. *Nature* 459, 393–397.
- (5) McIntosh, L. P., et al. (1996) The pKa of the General Acid/Base Carboxyl Group of a Glycosidase Cycles during Catalysis: A 13C-NMR Study of *Bacillus circulans* Xylanase. *Biochemistry* 35, 9958–9966.
- (6) Harris, T. K., and Turner, G. J. (2002) Structural Basis of Perturbed pKa Values of Catalytic Groups in Enzyme Active Sites. *IUBMB Life* 53, 85–98.
- (7) Chimentì, M. S., Castañeda, C. A., Majumdar, A., and García-Moreno E, B. (2011) Structural Origins of High Apparent Dielectric

Constants Experienced by Ionizable Groups in the Hydrophobic Core of a Protein. *J. Mol. Biol.* 405, 361–377.

(8) Isom, D. G., Castañeda, C. A., Cannon, B. R., and García-Moreno E, B. (2011) Large shifts in pKa values of lysine residues buried inside a protein. *Proc. Natl. Acad. Sci. U. S. A.* 108, 5260–5265.

(9) Shi, C., Wallace, J. A., and Shen, J. K. (2012) Thermodynamic Coupling of Protonation and Conformational Equilibria in Proteins: Theory and Simulation. *Biophys. J.* 102, 1590–1597.

(10) Fitch, C. A., Whitten, S. T., Hilser, V. J., and García-Moreno E, B. (2006) Molecular mechanisms of pH-driven conformational transitions of proteins: Insights from continuum electrostatics calculations of acid unfolding. *Proteins: Struct., Funct., Genet.* 63, 113–126.

(11) Harms, M. J., et al. (2008) A buried lysine that titrates with a normal pKa: Role of conformational flexibility at the protein–water interface as a determinant of pKa values. *Protein Sci.* 17, 833–845.

(12) Harms, M. J., et al. (2009) The pKa Values of Acidic and Basic Residues Buried at the Same Internal Location in a Protein Are Governed by Different Factors. *J. Mol. Biol.* 389, 34–47.

(13) Chimentì, M. S., et al. (2012) Structural Reorganization Triggered by Charging of Lys Residues in the Hydrophobic Interior of a Protein. *Structure* 20, 1071–1085.

(14) Grzesiek, S., and Dencher, N. A. (1986) Time-course and stoichiometry of light-induced proton release and uptake during the photocycle of bacteriorhodopsin. *FEBS Lett.* 208, 337–342.

(15) Heberle, J., and Dencher, N. A. (1992) Surface-bound optical probes monitor protein translocation and surface potential changes during the bacteriorhodopsin photocycle. *Proc. Natl. Acad. Sci. U. S. A.* 89, 5996–6000.

(16) Heberle, J. in *Biophysical and Structural Aspects of Bioenergetics* (Wikström, M., Ed.) pp 249–272, Royal Society of Chemistry, Cambridge, 2005.

(17) Whitten, S. T., García-Moreno E, B., and Hilser, V. J. (2005) Local conformational fluctuations can modulate the coupling between proton binding and global structural transitions in proteins. *Proc. Natl. Acad. Sci. U. S. A.* 102, 4282–4287.

(18) Lane, T. J., Shukla, D., Beauchamp, K. A., and Pande, V. S. (2013) To milliseconds and beyond: challenges in the simulation of protein folding. *Curr. Opin. Struct. Biol.* 23, 58–65.

(19) Hamelberg, D., Mongan, J., and McCammon, J. A. (2004) Accelerated molecular dynamics: A promising and efficient simulation method for biomolecules. *J. Chem. Phys.* 120, 11919–11929.

(20) Karp, D. A., et al. (2007) High Apparent Dielectric Constant Inside a Protein Reflects Structural Reorganization Coupled to the Ionization of an Internal Asp. *Biophys. J.* 92, 2041–2053.

(21) Goh, G. B., Laricheva, E. N., and Brooks, C. L. (2014) Uncovering pH-Dependent Transient States of Proteins with Buried Ionizable Residues. *J. Am. Chem. Soc.* 136, 8496–8499.

(22) Goddard, T. D., and Kneller, D. G. *Sparky 3*, University of California, San Francisco.

(23) Hansen, D. F., Vallurupalli, P., and Kay, L. E. (2008) An Improved 15N Relaxation Dispersion Experiment for the Measurement of Millisecond Time-Scale Dynamics in Proteins. *J. Phys. Chem. B* 112, 5898–5904.

(24) Morin, S., et al. (2014) relax: the analysis of biomolecular kinetics and thermodynamics using NMR relaxation dispersion data. *Bioinformatics* 30, 2219–2220.

(25) Carver, J. P., and Richards, R. E. (1972) A general two-site solution for the chemical exchange produced dependence of T2 upon the carr-Purcell pulse separation. *J. Magn. Reson.* 6, 89–105.

(26) Farrow, N. A., Zhang, O., Forman-Kay, J. D., and Kay, L. E. (1994) A heteronuclear correlation experiment for simultaneous determination of 15N longitudinal decay and chemical exchange rates of systems in slow equilibrium. *J. Biomol. NMR* 4, 727–734.

(27) Pérez, F., and Granger, B. E. (2007) IPython: A System for Interactive Scientific Computing. *Comput. Sci. Eng.* 9, 21–29.

(28) McKinney, W. Data Structures for Statistical Computing in Python, in *Proceedings of the 9th Python in Science Conference* (van der

Walt, S., and Millman, J., Eds.) pp 51– 56, Austin, Texas, June 28–July 3, 2010.

(29) van der Walt, S., Colbert, S. C., and Varoquaux, G. (2011) The NumPy Array: A Structure for Efficient Numerical Computation. *Comput. Sci. Eng.* 13, 22–30.

(30) Hunter, J. D. (2007) Matplotlib: A 2D Graphics Environment. *Comput. Sci. Eng.* 9, 90–95.

(31) Millet, O., Loria, J. P., Kroenke, C. D., Pons, M., and Palmer, A. G. (2000) The Static Magnetic Field Dependence of Chemical Exchange Linebroadening Defines the NMR Chemical Shift Time Scale. *J. Am. Chem. Soc.* 122, 2867–2877.

(32) Tollinger, M., Skrynnikov, N. R., Mulder, F. A. A., Forman-Kay, J. D., and Kay, L. E. (2001) Slow Dynamics in Folded and Unfolded States of an SH3 Domain. *J. Am. Chem. Soc.* 123, 11341–11352.

(33) Baldwin, A. J. (2014) An exact solution for $R_{2,eff}$ in CPMG experiments in the case of two site chemical exchange. *J. Magn. Reson.* 244, 114–124.

(34) Dyson, H. J., and Wright, P. E. (1998) Equilibrium NMR studies of unfolded and partially folded proteins. *Nat. Struct. Biol.* 5, 499–503.

(35) Baum, J., Dobson, C. M., Evans, P. A., and Hanley, C. (1989) Characterization of a partly folded protein by NMR methods: studies on the molten globule state of guinea pig α -lactalbumin. *Biochemistry* 28, 7–13.

(36) Lee, K. K., Fitch, C. A., Lecomte, J. T. J., and García-Moreno E, B. (2002) Electrostatic Effects in Highly Charged Proteins: Salt Sensitivity of pKa Values of Histidines in Staphylococcal Nuclease. *Biochemistry* 41, 5656–5667.

(37) Baran, K. L., et al. (2008) Electrostatic Effects in a Network of Polar and Ionizable Groups in Staphylococcal Nuclease. *J. Mol. Biol.* 379, 1045–1062.

(38) Castañeda, C. A., et al. (2009) Molecular determinants of the pKa values of Asp and Glu residues in staphylococcal nuclease. *Proteins: Struct., Funct., Genet.* 77, 570–588.

(39) Richman, D. E., Majumdar, A., and García-Moreno E, B. (2014) pH dependence of conformational fluctuations of the protein backbone. *Proteins: Struct., Funct., Genet.* 82, 3132–3143.

(40) Shaw, D. E., et al. (2008) Anton, a Special-purpose Machine for Molecular Dynamics Simulation. *Commun. ACM* 51, 91–97.

(41) Di Russo, N. V., Estrin, D. A., Martí, M. A., and Roitberg, A. E. (2012) pH-Dependent Conformational Changes in Proteins and Their Effect on Experimental pKas: The Case of Nitrophorin 4. *PLoS Comput. Biol.* 8, e1002761.